Langmuir
Letter
pubs.acs.org/Langmuir
© 2010 American Chemical Society

Self-Assembled Organic−Inorganic Hybrid Nanocomposite of a Perylenetetracarboxylic Diimide Derivative and CdS

Yanli Chen,*[,†] Lina Chen,[†] Guiju Qi,[†] Haixia Wu,[‡] Yuexing Zhang,[§] Lin Xue,[‡] Peihua Zhu,[†] Pan Ma,[‡] and Xiyou Li*[,‡]

[†]*School of Chemistry and Chemical Engineering, Shandong Provincial Key Laboratory of Fluorine Chemistry and Chemical Materials, University of Jinan, Jinan 250022, China,* [‡]*Department of Chemistry, Shandong University, Jinan 250100, China, and* [§]*Department of Chemistry, University of Science and Technology Beijing, Beijing 100083, China*

Received August 19, 2009. Revised Manuscript Received June 27, 2010

A perylenetetracarboxylic diimide derivative, *N*-*n*-hexyl-*N*′-(2-hydroxyethyl)-1,7-di(4′-*t*-butyl)phenoxy-perylene-3,4:9,10-tetracarboxylic diimide (**HO-PDI**), was synthesized and self-assembled as a monolayer thin solid film on the modified surface of a quartz substrate by an ester bond between −OH groups of **HO-PDI** molecules and −COOH groups of *p*-phthalic acid grafted onto the hydrophilic pretreated SiO_2 surface. An analysis of the spectral change revealed the *J*-aggregate nature of **HO-PDI** molecules in the obtained thin solid film. With this thin solid film of **HO-PDI** as a template, CdS nanoparticles were deposited on it in situ, which were further characterized by electronic absorption, fluorescence, and energy-dispersive X-ray spectroscopy (EDS). The morphology of CdS nanoparticles is disklike, and the diameter is ca. 140 nm as determined by atomic force microscopy (AFM). Furthermore, electron transfer between the organic layer and CdS nanoparticles was deduced through fluorescence quenching and theoretical analysis.

Introduction

Organic−inorganic nanocomposite material has been widely recognized as one of the most promising and rapidly emerging research areas for advanced materials with desirable optical, electrical, and magnetic properties.[1−6] The combined unique properties offered by both organic and inorganic components on a nanoscale level make such nanocomposites attractive for a wide range of applications including next-generation optics,[1] optoelectronic nanodevices,[2] thin-film field-effect transistors,[3] chemical or biological sensors, and catalysts.[4] The engineering of inorganic surfaces by the covalent bonding of organic molecules represents an interesting approach to the synthesis of hybrid inorganic/organic nanomaterials.[7] The use of SiO_2/Si,[8] Si(100),[9] or indium tin oxide (ITO) glass substrates[10] is particularly interesting from the perspective of optoelectronic device fabrication because of their ease of integration within electronic circuits. There have also been many reports on the hybrid films of organic/inorganic nanoparticles of CdSe,[5] CdS,[6] TiO_2,[11] Au,[12] ZrO_2,[13] and MoS_2[14] in which the inorganic and organic components interact through hydrogen bonding, van der Waals contacts, or electrostatic forces.

However, the self-assembly technique has recently emerged as a powerful technique for fabricating functional organic molecules into ultrathin solid films with controlled thickness and molecular architecture depending on various noncovalent interactions including $\pi-\pi$ interactions, van der Waals forces, hydrogen bonding, hydrophilic/hydrophobic interactions, electrostatic forces, and metal−ligand coordination.[15] As an important functional dye with outstanding photo and chemical stability as well as interesting photophysical and photochemical properties, perylenetetracarboxylic diimide derivatives (PDIs) have been intensively studied for several decades.[16−20] Because of their great potential application as organic semiconductors in different molecular electronic devices, the fabrication of ordered thin solid films of this functional molecular material has become an attracting research area in the past decade. However, the PDI thin solid films fabricated using either vapor deposition or Langmuir−Blodgett (LB) methods,[10,21]

*Corresponding authors. E-mail: chm_chenyl@ujn.edu.cn, xiyouli@sdu.edu.cn.

(1) Bi, W.; Louvain, N.; Mercier, N.; Luc, J.; Rau, I.; Kajzar, F.; Sahraoui, B. *Adv. Mater.* **2008**, *20*, 1013.
(2) Kira, A.; Umeyama, T.; Matano, Y.; Yoshida, K.; Isoda, S.; Isosomppi, M.; Tkachenko, N. V.; Lemmetyinen, H.; Imahori, H. *Langmuir* **2006**, *22*, 5497.
(3) Kagan, C. R.; Mitzi, D. B.; Dimitrakopoulos, C. D. *Science* **1999**, *286*, 945.
(4) Nishimura, A.; Sagawa, N.; Uchino, T. *J. Phys. Chem. C* **2009**, *113*, 4260.
(5) (a) Hu, L.; Zhao, Y.-L.; Ryu, K.; Zhou, C.; Stoddart, J. F.; Grüner, G. *Adv. Mater.* **2008**, *20*, 939. (b) Hao, E.; Wang, L.; Zhang, J.; Yang, B.; Zhang, X.; Shen, J. *Chem. Lett.* **1999**, *1*, 5.
(6) (a) Sheeney-Haj-Ichia, L.; Basnar, B.; Willner, I. *Angew. Chem., Int. Ed.* **2005**, *44*, 78. (b) Kotov, N. A.; Dekany, I.; Fendler, J. H. *J. Phys. Chem.* **1995**, *99*, 13065.
(7) Gulino, A.; Lupo, F.; Condorelli, G. G.; Mineo, P.; Fragala, I. *Chem. Mater.* **2007**, *19*, 5102.
(8) (a) Chen, Y.; Su, W.; Bai, M.; Jiang, J.; Li, X.; Liu, Y.; Wang, L.; Wang, S. *J. Am. Chem. Soc.* **2005**, *127*, 15700. (b) Gulino, A.; Mineo, P.; Scamporrino, E.; Vitalini, D.; Fragala, I. *Chem. Mater.* **2004**, *16*, 1838.
(9) Liu, Z.; Yasseri, A. A.; Lindsey, J. S.; Bocian, D. F. *Science* **2003**, *302*, 1543.
(10) Schroeder, R.; Ullrich, B. *Appl. Phys. Lett.* **2002**, *81*, 556.
(11) (a) Tadanaga, K.; Morinaga, J.; Matsuda, A.; Minami, T. *Chem. Mater.* **2000**, *12*, 590. (b) Liu, J. F.; Yang, K. Z.; Lu, Z. H. *J. Am. Chem. Soc.* **1997**, *119*, 11061.
(12) Cassagneau, T.; Fendler, J. H.; Mallouk, T. E. *Langmuir* **2000**, *16*, 241.
(13) Kang, E.-H.; Jin, P.; Yang, Y.; Sun, J.; Shen, J. *Chem. Commun.* **2006**, 4332.
(14) Tachibana, H.; Yamanaka, Y.; Sakai, H.; Abe, M.; Matsumoto, M. *Chem. Mater.* **2000**, *12*, 854.
(15) (a) Elemans, J . A. A. W.; Hameren, R. van; Nolte, R. J. M.; Rowan, A. E. *Adv. Mater.* **2006**, *18*, 1251. (b) Zang, L.; Che, Y.; Moore, J. S. *Acc. Chem. Res.* **2008**, *41*, 1596. (c) Lu, G.; Chen, Y.; Zhang, Y.; Bao, M.; Bian, Y.; Li, X.; Jiang, J. *J. Am. Chem. Soc.* **2008**, *130*, 11623.
(16) Jones, B. A.; Ahrens, M. J.; Yoon, M.-H.; Facchetti, A.; Marks, T. J.; Wasielewski, M. R. *Angew. Chem., Int. Ed.* **2004**, *43*, 6363.
(17) Gregg, B. A.; Cormier, R. A. *J. Am. Chem. Soc.* **2001**, *123*, 7959.
(18) Struijk, C. W.; Sieval, A. B.; J. Dakhorst, E. J.; van Dijk, M.; Kimkes, P.; Koehorst, R. B. M.; Donker, H.; Schaafsma, T. J.; Picken, S. J.; van de Craats, A. M.; Warman, J. M.; Zuihof, H. E.; Sudholter, J. R. *J. Am. Chem. Soc.* **2000**, *122*, 11057.
(19) Ranke, P.; Bleyl, I.; Simmerer, J.; Haarer, D.; Bacher, A.; Schmidt, H. W. *Appl. Phys. Lett.* **1997**, *71*, 1332.
(20) Li, X.; Sinks, L. E.; Rybtchinski, B.; Wasielewski, M. R. *J. Am. Chem. Soc.* **2004**, *126*, 10810.
(21) (a) Conboy, J. C.; Olson, E. J. C.; Adams, D. M.; Kerimo, J.; Zaban, A.; Gregg, B. A.; Barbara, P. F. *J. Phys. Chem. B* **1998**, *102*, 4516. (b) Schlettwein, D.; Back, A.; Schilling, B.; Fritz, T.; Armstrong, N. R. *Chem. Mater.* **1998**, *10*, 601. (c) Aroca, R.; Del Cano, T.; de Saja, J. A. *Chem. Mater.* **2003**, *15*, 38. (d) Dutta, A. K.; Vanoppen, P.; Jeuris, K.; Grim, P. C. M.; Pevenage, D.; Salesse, C.; De Schryver, F. C. *Langmuir* **1999**, *15*, 607. (e) Parra, V.; Del Cano, T.; Rodriguez-Mendez, M. L.; de Saja, J. A.; Aroca, R. F. *Chem. Mater.* **2004**, *16*, 358. (f) Chen, Y.; Kong, Y.; Wang, Y.; Ma, P.; Bao, M.; Li, X. *J. Colloid Interface Sci.* **2009**, *330*, 421.

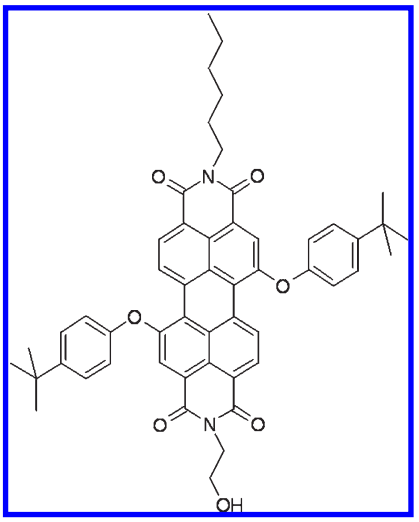

Figure 1. Molecular structure of **HO-PDI**.

depending mainly on the relatively weak intermolecular interactions, are easily disassembled by outer stimulation such as high temperature or organic solvent. As a result, for the purpose of practical applications, it is essential to have these PDIs organic films with high thermal stability and low solubility in most of the solvents. In this regard, Brochsztain et al. successfully fabricated an ordered thin solid film of *N*,*N*′-bis(2-phosphonoethyl)-3,4,9,10-perylenetetracarboxylic diimide (PPDI) supported by zirconium phosphonate. Because of the covalent bond between the PPDI molecules and the inorganic substrate, the resulting thin film had high stability.[22] Blanchard and co-worker reported on the covalent attachment of perylenedodecanoic acid and perylenetetracarboxylic acid at the silicon or indium tin oxide surface and their spectroscopic and electrochemical properties.[23] By means of the thiol linker, Würthner has successfully attached the self-assembled bis-perylenebisimide disulfide on a gold surface.[24] In this letter, we report on a novel two-step approach to the fabrication of an organic/inorganic hybride thin film composed of PDI and CdS, which involves the covalent immobilization of *N*-(*n*-hexyl)-*N*′-(2-hydroxyethyl)-1,7- di(4′-*t*-butyl)-phenoxy-perylene-3,4:9,10- tetracarboxylic diimide (**HO-PDI**, Figure 1) on a quartz surface and the in situ deposition of CdS nanoparticles on the thin solid film of surface-bound **HO-PDI**. The resulting **HO-PDI** monolayers and CdS/**HO-PDI** hybrid films have been characterized via electronic absorption and fluorescence spectra, atomic force microscopy (AFM), and energy-dispersive X-ray spectroscopy (EDS). Significant fluorescent quenching can be detected in this hybrid system, indicating the presence of a strong interaction between the organic layer and inorganic nanoparticles. This research provided a new way to preparing given organic and inorganic nanostructures with a controlled molecular packing mode, which might find potential applications in optoelectronic devices.

Experimental Section

Reagents and Apparatus. The *N*-(*n*-hexyl)-*N*′-(2-hydroxyethyl)-1,7-di(4′-*t*-butyl) phenoxy-perylene-3,4:9,10-tetracarboxylic diimide (**HO-PDI**) was synthesized and purified according to published procedures.[25,26] The detailed synthesis procedures together with the structural characterization are described in the Supporting Information. Dicyclohexyl carbodimide (DCC) was purchased from Aldrich. Dichloromethane for the preparation of self-assembled (SA) films of **HO-PDI** was freshly distilled from CaH_2 under nitrogen. Other reagents are used as received without further purification unless there is specific notation. Electronic absorption spectra were recorded on a Hitachi U-4100 spectrophotometer. The fluorescence spectra were measured on an ISIS K2 system. AFM images were collected in air under ambient conditions using tapping mode with a Nanoscope III/Bioscope scanning probe microscope from Digital Instruments. Chemical compositions of the organic−inorganic hybrid nanocomposite were studied by energy-dispersive spectrometry (EDS) with an Oxford INCA X-sight instrument. Electrochemical measurements for **HO-PDI** solution were carried out with a BAS CV-50W voltammetric analyzer, and the detailed experimental process can be found in Supporting Information.

Preparation of the HO-PDI SA Film. A mixture of *p*-phthalic acid (1.3 mg, 0.0078 mmol) and DCC (1.6 mg, 0.0078 mmol) was dissolved in 5 mL of bromobenzene (solution 1). Another mixture of **HO-PDI** (6.35 mg, 0.0078 mmol) and DCC (1.6 mg, 0.0078 mmol) was dissolved in 5 mL of dichloromethane (solution 2). The preparation of the thin film required a three-step procedure (Scheme 1): (i) Quartz substrates were hydrophilically pretreated according to the published procedures.[8b] Substrates were first cleaned with piranha solution (H_2SO_4/30% H_2O_2 70:30 v/v) at 80 °C for 1 h. ***Caution!*** *Piranha solution is an extremely strong oxidizing reagent*. Then they were repeatedly rinsed with doubly distilled water and immersed in an H_2O/30% H_2O_2/NH_3 5:1:1 v/v/v mixture at room temperature for 40 min, washed again with doubly distilled water, and dried under vacuum just before the deposition of the coupling reagent. (ii) The newly treated quartz substrates were immersed in solution 1 at room temperature for 12 h to afford a monolayer of the coupling reagent. Then, they were washed with copious amounts of bromobenzene and cleaned ultrasonically in acetone for 1 min to remove any physically adsorbed coupling reagent. (iii) The substrates bearing the covalently bound *p*-phthalic acid were immersed in solution 2 for 24 h to bond **HO-PDI** molecules. Finally, the substrates bearing the covalently bonded **HO-PDI** molecules were repeatedly washed with dichloromethane to remove any residual unreacted **HO-PDI**, which resulted in a self-assembly film of **HO-PDI** (template 1).

Preparation of CdS Nanoparticles on the Modified HO-PDI SA Film. Template 1 was dipped into a $CdCl_2$ aqueous solution (0.14 mmol/L) for 12 h. After being washed with water, the thin film was subjected to drying in air. The dried film was placed in an atmosphere of H_2S gas liberated from a thioacetamide aqueous solution at reduced pressure (Scheme 1).

Results and Discussion

To connect PDI to the surface of SiO_2 covalently, a novel PDI derivative, namely, *N*-(*n*-hexyl)-*N*′-(2-hydroxyethyl)-1,7-di(4′-*t*-butyl)phenoxy-perylene-3,4:9,10 -tetracarboxylic diimide (**HO-PDI**, Figure 1) was designed and prepared. The introduction of functional groups having rich electron-donor units on the perylene backbone is expected to improve its solubility in conventional organic solvents. The hydroxyethyl unit and hydrophobic linear alkyl chain linked at the imide nitrogen positions provide sufficient flexibility for the optimization of both reactions of **HO-PDI** with SiO_2-supported *p*-phthalic acid and the noncovalent stacking of the perylene diimide π systems. The detailed synthesis procedures together with the structure characterization are described in Supporting Information.

Electronic absorption and steady-state fluorescence spectra are sensitive to the interchromophore distance and orientation[27,28]

(22) Marcon, R. O.; dos Santos, J. G.; Figueiredo, K. M.; Brochsztain, S. *Langmuir* **2006**, *22*, 1680.
(23) Mazur, M.; Blanchard, G. J. *Langmuir* **2005**, *21*, 1441.
(24) Haas, U.; Thalacker, C.; Adams, J.; Fuhrmann, J.; Riethmüller, S.; Beginn, U.; Ziener, U.; Moller, M.; Dobrawa, R.; Würthner, F. *J. Mater. Chem.* **2003**, *13*, 767.
(25) Zhao, C.; Zhang, Y.; Li, R.; Li, X.; Jiang, J. *J. Org. Chem.* **2007**, *72*, 2402.
(26) Wang, Y.; Chen, Y.; Li, R.; Wang, S.; Su, W.; Ma, P.; Wasielewski, M. R.; Li, X.; Jiang, J. *Langmuir* **2007**, *23*, 5836.
(27) Kazmaier, P. M.; Hoffmann, R. *J. Am. Chem. Soc.* **1994**, *116*, 9684.
(28) Johnson, E.; Aroca, R. *Langmuir* **1995**, *11*, 1693.

Scheme 1. Procedures for the Fabrication of the Hybrid CdS/HO-PDI SA Film

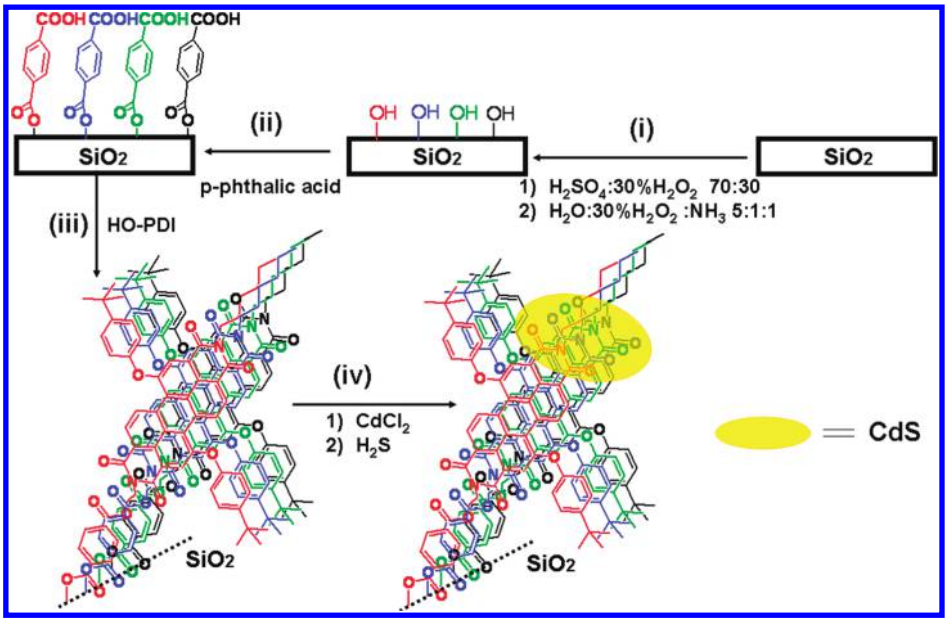

and have been widely used to study the nature of the molecular self-assembly of dyes.[28−33] The absorption and fluorescence spectra of **HO-PDI** in CH_2Cl_2 solution are shown in Figure 2A. The absorption spectrum of **HO-PDI** in solution showed two absorption maxima at 549 and 513 nm, which correspond to 0−0 and 0−1 vibrational band of the S_0-S_1 transition, respectively. The observed absorption band around 404 nm is attributed to the electronic S_0-S_2 transition.[34,35] The fluorescence spectrum of the same solution is a mirror image of the S_0-S_1 absorption band, giving no indication of aggregation in dichloromethane.[33] The peak positions of both the absorption and fluorescence of **HO-PDI** correspond well to those of known PDIs with a similar substitution pattern at the bay positions.[33,34] Compared to that of dichloromethane solution, the absorption spectrum of the **HO-PDI** SA film in Figure 2B shows an intensely red-shifted component with a broad maximum at 628 nm and a blue-shifted component at 496 nm. The dramatic changes in the electronic transitions are indicative of intermolecular dipole−dipole interaction between the perylene rings[27] and thus the aggregation of the molecules. Kasha's point-dipole model provides a rationale for the observed band shifts and the split. The extreme case is represented by a head-to-tail arrangement of the dipoles, which results in a red-shifted band (J aggregate), and a blue-shifted band arises from a parallel arrangement of the dipoles (H aggregate).[36] The strong red- and blue-shifted band components observed in the absorption spectrum of the SA film represent an intermediate

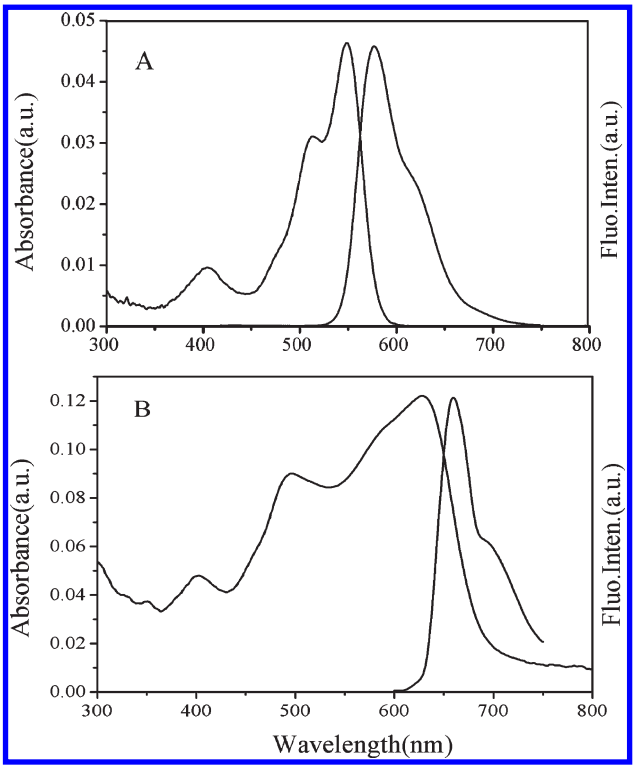

Figure 2. Electronic absorption (left) and fluorescence (right) spectra of (A) **HO-PDI** in solution and (B) **HO-PDI** SA film. The excitation wavelength was 410 nm.

case that results in apparent band splitting and is conventionally thought of as a slipped cofacial stack with an "edge-on" configuration on the surface of the substrate.[31,37,38] Compared to that in solution, the half bandwidth of the absorption bands of **HO-PDI** SA film increased dramatically (Figure 2B), indicating a slipped cofacial arrangement between adjacent perylene chromophores of the **HO-PDI** molecules (Scheme 1). This phenomenon has also

(29) Yan, P.; Chowdhury, A.; Holman, M. W.; Adams, D. M. *J. Phys. Chem. B* **2005**, *109*, 724.
(30) Van der Boom, T.; Hayes, R. T.; Zhao, Y.; Bushard, P. J.; Weiss, E. A.; Wasielewski, M. R. *J. Am. Chem. Soc.* **2002**, *124*, 9582.
(31) Iverson, I. K.; Casey, S. M.; Seo, W.; Tam-Chang, S.-W.; Pindzola, B. A. *Langmuir* **2002**, *18*, 3510.
(32) Struijk, C. W.; Sieval, A. B.; Dakhorst, J. E. J.; van Dijk, M.; Kimkes, P.; Koehorst, R. B. M.; Donker, H.; Schaafsma, T. J.; Picken, S. J.; van de Craats, A. M.; Warman, J. M.; Zuilhof, H.; Sudhölter, E. J. R. *J. Am. Chem. Soc.* **2000**, *122*, 11057.
(33) Würthner, F.; Thalacker, C.; Diele, S.; Tschierske, C. *Chem.—Eur. J.* **2001**, *7*, 2245.
(34) Vajiravelu, S.; Ramunas, L.; Vidas, G. J.; Valentas, G.; Vygintas, J.; Valiyaveettil, S. *J. Mater. Chem.* **2009**, *19*, 4268.
(35) Chao, C. C.; Leung, M. K.; Su, Y. O.; Chiu, K. Y.; Lin, T. H.; Shieh, S. J.; Lin, T. H. *J. Org. Chem.* **2005**, *70*, 4323.
(36) Kasha, M.; Rawls, H. R.; El-bayoumi, M. A. *Pure Appl. Chem.* **1965**, *11*, 371.
(37) Czikklely, V.; Forsterling, H. D.; Kuhn, H. *Chem. Phys. Lett.* **1970**, *6*, 207.
(38) Nagata, N.; Kugimiya, S.; Kobuke, Y. *Chem. Commun.* **2000**, 1389.

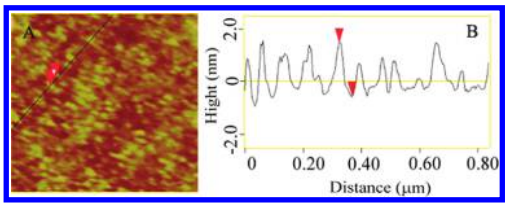

Figure 3. (A) Morphology of the **HO-PDI** SA film captured by AFM (scan range = $1 \times 1\ \mu m^2$; height scale = 5 nm) and (B) corresponding section analysis of the **HO-PDI** SA film.

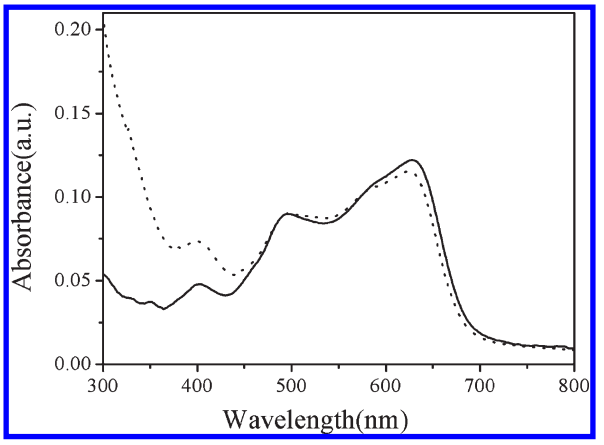

Figure 4. Comparison of the difference electronic absorption spectra of the CdS/**HO-PDI** SA film (· · ·) and the **HO-PDI** SA film (−) .

been observed previously for the porphyrin aggregates with a slipped cofacial oriented structure, where two transition moments interact in face-to-face and parallel orientation to give rise to blue and red shifts, respectively, leading to the observed band broadening.[38,39] The emission spectrum of the **HO-PDI** SA film showed a significant red shift (about 80 nm) of the emission maxima upon aggregation. The emission maxima in the longer-wavelength region as compared to that in solution should be attributed to emission from the low-energy exciton state of J aggregates formed by the interaction between adjacent HO-PDI molecules in the slipped cofacial arrangement. This result is in good agreement with a study on thin films of analogous PDI derivatives reported by Würthner and co-workers.[33]

The surface morphology of the **HO-PDI** SA film was obtained by atomic force microscopy (AFM) measurement, as shown in Figure 3A. Elongated domains can be observed in the image. It is worth noting that the morphology of the **HO-PDI** SA film is not homogeneous because of self-aggregation of the **HO-PDI** molecules in the SA film. The widths of elongated domains are in the range of 30−50 nm, and the lengths are in the range of about 60−150 nm. The thickness of the **HO-PDI** SA film is about 2.0 nm (Figure 3B), which is shorter than the total length of a **HO-PDI** molecule bonded to the *p*-phthalic acid by ester bond, 2.8 nm, which is obtained from the energy-optimized structure of the molecule using PCMODEL. This is likely due to the tilted stacking of **HO-PDI** planes with respect to the quartz substrate surface, in line with the strong hydrophobic interaction between side chains, which usually results in effective side-chain interdigitation and thus leads to a shortened length along the longitudinal direction.[40]

With the above **HO-PDI** SA film as a template, the CdS nanoparticles were deposited. By comparing the electronic absorption spectra of the CdS/**HO-PDI** SA film (dotted line in Figure 4) and the **HO-PDI** SA film (solid line in Figure 4), one can see that the CdS/**HO-PDI** SA film exhibits a higher absorption intensity in the wavelength region below 450 nm, which is very similar to the absorption of core-embedded CdS nanoparticles, the TBP-stabilized CdS film, and alkylated dendrimer-stabilized CdS nanoplatelets[41−43] but different from that of bulk CdS material (the absorption edge is near 590 nm).[44] However, the 0−0 and 0−1 peaks of the **HO-PDI** SA film and the CdS/**HO-PDI** SA film did not show a significant change, suggesting similar packing behavior of **HO-PDI** molecules in a covalently attached monolayer before and after CdS nanoparticles deposition.

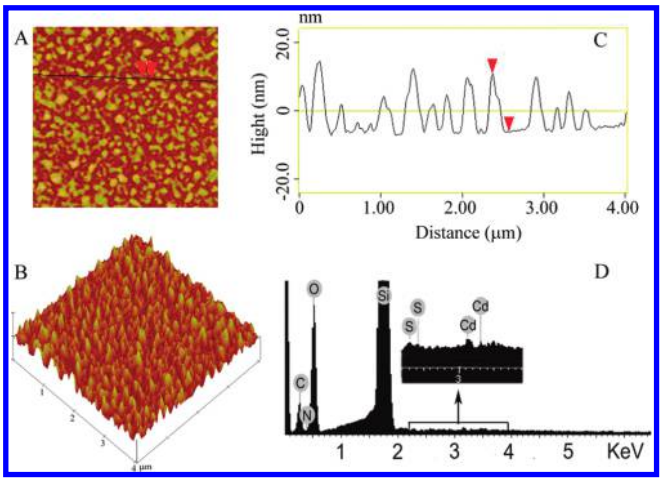

Figure 5. (A) AFM phase image (scan range $4 \times 4\ \mu m^2$, height scale 40 nm), (B) AFM 3D image, (C) corresponding section analysis of the CdS nanoparticles on the modified **HO-PDI** SA film, and (D) EDS of the CdS nanoparticles deposited on the **HO-PDI** SA film.

The AFM images were also captured after CdS deposition (Figure 5A). The morphology of the hybrid thin solid film is quite different from that of the **HO-PDI** SA film. By comparing the two images, it can be seen directly that CdS nanoparticles are grown on the surface of the **HO-PDI** SA film with monodisperse dimensions (Figure 5B). The average grain diameter is around 140 nm, which can be rationalized in terms of the period of the organic domains. As shown in Figure 5C, the average thickness of the CdS nanoparticles on the modified **HO-PDI** SA film is ca. 20 nm. Considering the thickness of the organic SA film (about 2.0 nm), the average thickness of the CdS nanoparticles on the **HO-PDI** SA film should be about 18 nm, which is much less than the average grain diameter; therefore, the disk shape is expected for the CdS nanoparticles. The success in preparing **HO-PDI** SA films modified by CdS nanoparticles was further confirmed by the elemental signatures of C, O, N, S, and Cd in the EDS as shown in Figure 5D. The atomic ratio of 1:1 for Cd versus S is indicative of the composite of the CdS nanoparticles.

To understand the growth model of CdS nanoparticles on the surface of the **HO-PDI** SA film, a natural bond orbital (NBO) calculation was used to analyze the charge distribution in the **HO-PDI** molecule (DFT calculation on the B3LYP/6-31G* level). From the NBO analysis of the **HO-PDI** molecule (Figure S1, Supporting Information), we can find that the negative charges are distributed mainly on oxygen and nitrogen atoms of the imide

(39) Kobuke, Y.; Miyaji, H. *J. Am. Chem. Soc.* **1994**, *116*, 4111.
(40) Balakrishnan, K.; Datar, A.; Naddo, T.; Huang, J.; Oitker, R.; Yen, M.; Zhao, J.; Zang, L. *J. Am. Chem. Soc.* **2006**, *128*, 7390.
(41) Zhao, H.; Douglas, E. P. *Chem. Mater.* **2002**, *14*, 1418.
(42) Schreder, B.; Schmidt, T.; Ptatschek, V.; Winkler, U.; Materny, A.; Umbach, E.; Lerch, M.; Muller, G.; Kiefer, W.; Spanhel, L. *J. Phys. Chem. B* **2000**, *104*, 1677.
(43) Donners, J. J. J. M.; Hoogenboom, R.; Schenning, A. P. H. J.; Hal, P. A.; Nolte, R. J. M.; Meijer, E. W.; Sommerdijk, N. A. J. M. *Langmuir* **2002**, *18*, 2571.
(44) Ray, B. *II-VI Compounds*; Pergamon Press: Oxford, U.K., 1969.

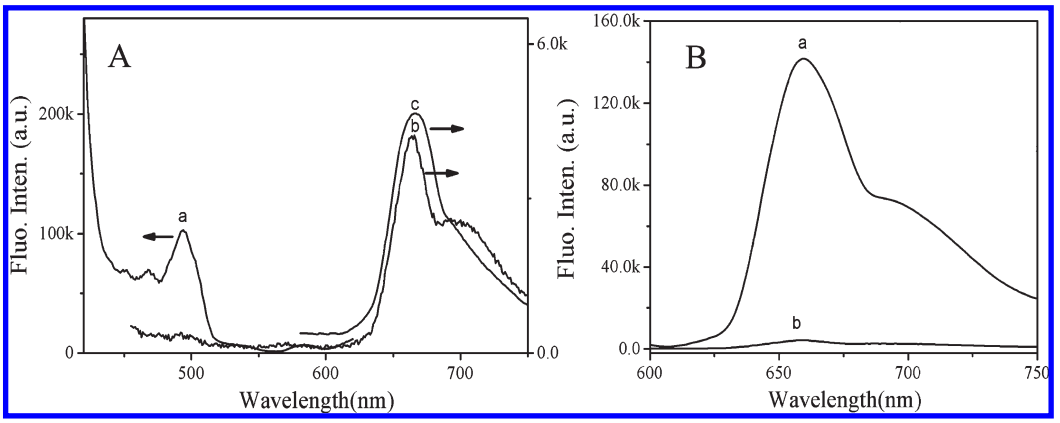

Figure 6. Fluorescence spectra of (A) the CdS/**HO-PDI** SA film upon excitation at 350 nm (line a), 410 nm (line b), and 550 nm (line c). (B) Comparison of the fluorescence emission spectra of the **HO-PDI** SA film (line a) and the CdS/**HO-PDI** SA film (line b) at λ_{ex} = 410 nm.

groups. Therefore, when the **HO-PDI** SA film is immersed in a $CdCl_2$ solution, Cd^{2+} should accumulate around the negatively charged oxygen and nitrogen atoms. Because the interaction between Cd^{2+} and oxygen or nitrogen atoms is an ion−polar interaction, it is weaker than electrostatic interactions and Cd^{2+} can move along the elongated domains of the HO-PDI self-assembly. Similar behavior has been reported for the synthesis of nanostructured CdS in which self-assembled nanoribbons of amphiphilic DRC molecules act as a direct template by confining the precursor ions to the hydrophilic regions of the ribbons.[45] When H_2S gas is introduced, Cd^{2+} has to diffuse along the elongated domains to form CdS nuclei. These nuclei grow until they eventually join to form a continuous solid, so the horizontal dimension of the diameter of the CdS nanoparticle is quite large (about 140 nm). However, the mobility of Cd^{2+} along the vertical direction of the SA film of **HO-PDI** is limited, which, together with the crystal lattice limitation of CdS, induces the formation of the disk-shaped CdS nanoparticles.

Because the CdS nanoparticles prepared in our system have a different shape from those prepared by conventional methods (spherical shape), it is interesting to study the interaction between the **HO-PDI** template and the CdS nanostructure. Fluorescence spectra of the CdS/**HO-PDI** SA film upon excitation at wavelengths of 350, 410, and 550 nm were recorded (Figure 6A). The emission spectrum upon excitation at 350 nm presents an emission maximum at 490 nm, which can be assigned to the emission of the CdS nanostructures.[41,43] However, an emission maximum at 664 nm with relatively weak intensity was observed when the hybrid film was excited at 410 or 550 nm, which should be attributed to the emission from **HO-PDI**.[26,46] Although the absorption edge of CdS particles is at about 450 nm (Figure 4), no emission from the CdS nanoparticles in the hybrid film has been detected upon excitation at 410 nm. The fluorescence spectra of the **HO-PDI** SA film before and after CdS nanoparticle deposition at the same excitation wavelength (λ_{ex} = 410 nm) are compared in Figure 6B. It has been found that the emission spectra do not change much in shape after CdS deposition but the intensity decreases remarkably. This indicates that the fluorescence of the **HO-PDI** SA film has been quenched after CdS nanoparticle deposition. The fluorescence quenching efficiency is calculated to be as high as 97%. The efficient fluorescence quenching might be induced by charge transfer or energy transfer between the **HO-PDI** molecules and CdS nanoparticles. As can be seen from Figure 4, the absorption of CdS nanoparticles in the region above 450 nm is very weak and the emission maximum for the **HO-PDI** SA film is centered at 660 nm (Figure 2B). There is no overlap between the emission band of **HO-PDI** and the absorption band of CdS; therefore, the energy transfer from **HO-PDI** to CdS nanoparticles is theoretically impossible. Because multiple reports in the literature indicate that the photoinduced electron transfer between CdS and organic dyes dominates the fluorescence quenching process,[5a,10,47] it is reasonable to assume that the fluorescence quenching in the present system proceeds by electron transfer between CdS and **HO-PDI**. According to this assumption, the charge-transfer process between CdS and **HO-PDI** can be depicted using the concept of energy-level matching. The HOMO and LUMO levels have been evaluated using cyclic voltammetry and differential pulse voltammetry (DPV).[34] The half-wave redox potential values versus SCE are summarized in Supporting Information, Table S1. A representative cyclic voltammogram and differential pulse voltammogram for **HO-PDI** are given in Figure S2. The HOMO and LUMO energy values for **HO-PDI** are −5.90 and −3.81 eV with respect to the zero-vacuum level, respectively, which can be inferred experimentally from the first one-electron oxidation and reduction process (Supporting Information) obtained for the electrochemical result.[34] However, the band gap of bulk cubic CdS is 2.4 eV with the conduction band (E_c) and valence band (E_v) at −4.1 and −6.5 eV, respectively, with respect to the vacuum energy level. These bulk material values are applicable to explaining the properties of small particles as confirmed by the previous report.[48] When **HO-PDI** molecules are excited, electrons of **HO-PDI** can be excited from the HOMO to the LUMO. The electron at the LUMO energy level of **HO-PDI** can easily transfer to the conducting band (E_c) of CdS (Scheme 2). The energy levels of **HO-PDI** (HOMO and LUMO) and CdS (E_v and E_c) are compatible for electron transfer with the **HO-PDI** molecule as the donor and the CdS nanoparticle as the acceptor.

PDIs are normally good electron acceptors in most of the electron donor−acceptor pairs, but their redox properties markedly depend on substituents in the so-called bay region. Electron-withdrawing substituents at the bay positions (e.g., −CN or −X) can enhance the electron affinity of PDIs[16,49] whereas the electron-donating

(45) Sone, E. D.; Zubarev, E. R.; Stupp., S. I. *Angew. Chem., Int. Ed.* **2002**, *41*, 1705.
(46) Feng, J.; Zhang, Y.; Zhao, C.; Li, R.; Xu, W.; Li, X.; Jiang, J. *Chem.—Eur. J.* **2008**, *14*, 7000–7010.
(47) Boulesbaa, A.; Issac, A.; Stockwell, D.; Huang, Z.; Huang, J.; Guo, J.; Lian, T. *J. Am. Chem. Soc.* **2007**, *129*, 15132.
(48) Hasselbarth, A.; Eychmiiller, A.; Weller, H. *Chem. Phys. Lett.* **1993**, *203*, 271.
(49) Briseno, A. L.; Mannsfeld, S. C. B.; Reese, C.; Hancock, J. M.; Xiong, Y.; Jenekhe, S. A.; Bao, Z.; Xia, Y. *Nano Lett.* **2007**, *7*, 2847.

Scheme 2. Electron-Transfer Mechanism between HO-PDI and CdS Nanoparticles

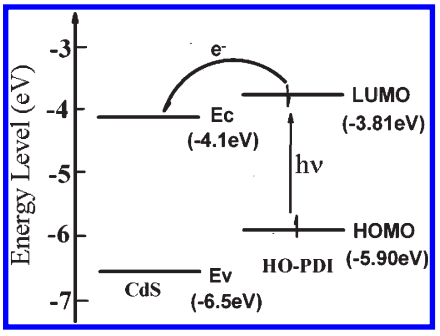

substituents (e.g., phenoxy or amino substituents) reduce the electron affinity of PDIs. The small electron affinity will favor an electron-donating process by lowering the HOMO−LUMO energy level and band gap.[34] Therefore, PDIs with electron-donating groups at bay positions can also be as an electron donor in some cases.[34,50−55] **HO-PDI** has electron donating phenoxyl groups at the bay positions, and it is possible to play an electron donor in this hybrid system. It is worth noting that the electron-transfer mechanism from **HO-PDI** to CdS is just a most probable speculation as this stage. To gain further insight into the mechanism of fluorescence quenching, direct observation of the reduced species of **HO-PDI** by time-resolved measurement is perhaps the most reliable method. However, such a measurement was proven to be very challenging because the transient absorption signals of the ultrathin film are too weak to be recorded.

In summary, a disk-shaped CdS nanostructure, which is different from the spherically shaped nanoparticles, has been successfully prepared. There exists a strong interaction between the CdS nanostructure and **HO-PDI** molecules. Charge transfer may take place with **HO-PDI** as the donor and CdS as the acceptor. This kind of composite film with an organic/inorganic hybrid structure should have potential applications in a photoelectric conversion system. It is believed to be helpful in opening new possibilities for the construction of molecularly based nanooptoelectronics.

Acknowledgment. Financial support from the Natural Science Foundation of China (grant no. 20871055), the Key Subject Research Foundation of Shandong Province (grant no. XTD0704), and the University of Jinan is gratefully acknowledged.

Supporting Information Available: Detailed synthesis procedures together with the structure characterization for **HO-PDI**. Electron distribution of the energy-optimized conformation of the **HO-PDI** molecule by natural bond orbital (NBO) calculation. Electrochemical measurements, typical representative cyclic voltammograms and differential pulse voltammograms, and experimental electrochemical data of **HO-PDI** in CH_2Cl_2. EDS spectrum of the **HO-PDI** SA film after the $CdCl_2$ step (before exposure to H_2S). Fluorescence spectra of the HO-PDI SA film upon excitation at 628 and 496 nm, respectively. This material is available free of charge via the Internet at http://pubs.acs.org.

(50) Finlayson, C. E.; Friend, R. H.; Otten, M. B. J.; Schwartz, E.; Cornelissen, J.J. L. M.; Nolte, R. J. M.; Rowan, A. E.; Samorí, P.; Palermo, V.; Liscio, A.; Peneva, K.; Müllen, K.; Trapani, S.; Beljonne, D. *Adv. Funct. Mater.* **2008**, *18*, 3947.
(51) Würthner, F. *Chem. Commun.* **2004**, 1564.
(52) Shibano, Y.; Umeyama, T.; Matano, Y.; Imahori, H. *Org. Lett.* **2007**, *9*, 1971.
(53) Shibano, Y.; Umeyama, T.; Matano, Y.; Tkachenko, N. V.; Lemmetyinen, H.; Imahori, H. *Org. Lett.* **2006**, *8*, 4425.
(54) Shibano, Y.; Umeyama, T.; Matano, Y.; Tkachenko, N. V.; Lemmetyinen, H.; Araki, Y.; Ito, O.; Imahori, H. *J. Phys. Chem. C* **2007**, *111*, 6133.
(55) Lukas, A. S.; Zhao, Y.; Miller, S. E.; Wasielewski, M. R. *J. Phys. Chem. B* **2002**, *106*, 1299.